Desalination and Water Treatment
www.deswater.com

doi: 10.5004/dwt.2022.28391

254 (2022) 208–216
April

Enhancement of corrosion inhibition efficiency of sodium alginate via grafting with polyacrylamide

Ahmed Hefnawy[a,b,*], Salma Hassan Zaki[c], Mohammed Salah El-Din Hassouna[c], Shacker Helmi[c]

[a]*Department of Chemistry, College of Science, University of Bahrain, Sakhir 32038, Kingdom of Bahrain, email: ahefnawy@uob.edu.bh/ahmed.hefnawy@alexu.edu.eg (A. Hefnawy)*
[b]*Department of Materials Science, Institute of Graduate Studies and Research, Alexandria University, P.O. Box 832, Egypt*
[c]*Department of Environmental Studies, Institute of Graduate Studies and Research, Alexandria University, 21526 Alexandria, Egypt, emails: igsr.salmazaki@alexu.edu.eg (S.H. Zaki), S_hassouna@alexu.edu.eg (M.S. El-Din Hassouna), igsr.shackerh@alexu.edu.eg (S. Helmi)*

Received 2 October 2021; Accepted 16 February 2022

ABSTRACT

Copolymerization of sodium alginate (SAG) with polyacrylamide (PAC) was successfully achieved using microwave assisted polymerization technique. At 240 mg/100 mL sodium alginate on its own gave an inhibition efficiency of 64%, while its grafting with polyacrylamide the efficiency reached 86%. Statistical analysis revealed a highly significant difference in inhibition efficiency between SAG and SAG-*g*-PAC. SAG-*g*-PAC data obeyed four adsorption isotherm models, namely Langmuir, Temkin, Flory–Huggins, and kinetic model of El-Awady isotherm, while SAG data obeyed only Langmuir model. Scanning electron microscopy images revealed the smoothness and homogeneity of SAG-*g*-PAC adsorption on the mild steel surface.

Keywords: Anticorrosion; Grafted sodium alginate; Polyacrylamide; Co-biopolymer; Adsorption isotherm

1. Introduction

Among all corrosion control approaches, the use of corrosion inhibitors is considered the most effective one for its low cost, easy to apply, and diversity. Recently, searching for low toxicity inhibitors with high inhibition efficiency gained a great interest [1–4]. Many authors reported the use of environmentally friendly inhibitory extracts of plant [5], animal [6], and microbial origin [7,8], such as essential oil of *Eryngium maritimum*, chitosan and sodium alginate. These inhibitors usually contain heteroatoms (O, N, S, P) in their chemical structure which provides various bonding sites on the metal surface forming an adsorbed layer isolating and protecting metal surface from interacting with corrosive media [9–12].

Alginate is an anionic polysaccharide extracted from brown algae. In addition to its various applications in food and pharmaceutical industries, sodium alginate has been reported as a corrosion inhibitor of different metals and alloys in different media [7,13–19]. Heteroatoms anchored in the polyacrylamide makes it a good corrosion inhibitor [20–22]. Grafting a synthetic polymer onto natural polysaccharides have been reported in several studies as to improve natural products inhibition efficiency. Polyacrylamide grafting polymerization has been widely reported in corrosion inhibition studies [23–29]. Microwave

* Corresponding author.

grafted polymerization is widely used for its higher grafting efficiency and saving reaction time [30].

The objective of this work is to synthesize and characterize sodium alginate grafted with polyacrylamide (SAG-*g*-PAC) as to be used as a highly efficient corrosion inhibitor. The experimental design for this study includes comparing the inhibition efficiency of sodium alginate with sodium alginate grafted with polyacrylamide in 0.1 M sulfuric acid medium using electrochemical measurements. In addition, morphological changes in the metal surface are investigated using scanning electron microscopy. Different adsorption isotherm models are to be tested in the case of the sodium alginate grafted with polyacrylamide.

2. Experimental

2.1. Chemicals

Sodium alginate (SAG) was obtained through a local agent from Oxford Lab Chemicals, India. Acrylamide, ammonium persulphate, sulfuric acid 98% were obtained from Elgomhouria Company, Egypt.

2.2. Synthesis of sodium alginate grafted with polyacrylamide

Sodium alginate grafted with polyacrylamide (SAG-*g*-PAC) was prepared according to the microwave-assisted free radical polymerization method using a 900 W domestic microwave [31]. Preparation details were as follows: in a 100 mL beaker 1 g sodium alginate was dissolved in 40 mL of distilled water, 7 g acrylamide were added and dissolved in the solution. This was followed by addition of 0.3 g of ammonium persulfate (APS) as an initiator, this solution was irradiated in a microwave for a total of 3 min; during this period the solution was cooled at time intervals in an ice box to avoid overheating. A gel like mass was formed and extracted with acetone; filtered off and dried in an oven at 60°C for 24 h. Afterwards, it was pulverized to be used as a corrosion inhibitor.

2.3. Characterization of the grafted bio-copolymer

Grafted bio-copolymer SAG-*g*-PAC was characterized using Fourier-transform infrared (FTIR, PerkinElmer spectrophotometer) in the range 4,000–500 cm^{-1}.

2.4. Preparation of electrochemical testing medium

Concentrated sulphuric acid was diluted with distilled water to prepare 0.1 M solution as a corrosion testing medium.

2.5. Preparation of the working electrode

A cylindrical rod steel of 1 cm covered all around with Teflon with a thickness of 0.5 cm was cut with a dimension of 2.5 cm length and 1.5 cm total diameter and 1.0 cm^2 cross surface area of the steel. The chemical composition of the steel, which was used as a working electrode, was analyzed at the Egyptian Copper Works, CO., Alexandria, Egypt using optical emission quantometer (Table 1). The electrode surface was polished using different grades of emery papers starting with coarse to fine one, then washed with distilled water and sonicated with acetone, just before being immersed in the corrosion medium. Then, corrosion rate was to measure corrosion rate electrochemically measured.

Table 1
Chemical composition of the steel specimen

Element	% weight
C	0.255
S	0.030
P	0.030
Mn	0.725
Si	0.120
Fe	98.840

2.6. Treatment

In testing corrosion inhibition efficiency of the two compounds SAG and SAG-*g*-PAC dosing was at 40, 160, 200, and 240 mg/100 mL acidic corrosion medium.

2.7. Electrochemical measurements

A multi necked electrochemical cell, 250 mL rounded bottom flask, the multiple necks were used for a steel electrode as the working electrode (WE), a platinum foil as the counter electrode (PE)/auxiliary electrode and a saturated calomel electrode (SCE) as the reference electrode. The corrosion inhibition efficiency of mild steel samples was determined on three samples as replicas using (DC) potentiodynamic polarization and electrochemical impedance spectroscopy (EIS). The DC potentiodynamic polarization and the impedance measurements were performed in the standard electrochemical cell. The electrochemical cell was connected to Gamry PC14G750 potentiostat/Galvanostat/ZRA analyzer, with a Gamry framework system based on ESA400 Gamry applications including DC 105 corrosion software, and EIS300 software and Echem Analyst 5.5 software for data plotting, graphing, data fitting, and calculation. Using DC potentiodynamic experiments were performed by scanning the electrode potential from −250 to +250 mV around E_{corr} at scan rate of 0.5 mV s^{-1}. The two tangent lines of Tafel plots about 50 mV around E_{corr} were extrapolated to calculate the polarization parameters anodic and cathodic current density slopes (β_A, β_C), corrosion potential (E_{corr}), corrosion current density (i_{corr}). The inhibition efficiency (%IE) was calculated using Eq. (1):

$$\text{IE\%} = \frac{i^{\circ}_{corr} - i_{corr}}{i^{\circ}_{corr}} \times 100 \quad (1)$$

where the parameters: i°_{corr} and i_{corr} are the corrosion current density in the absence and the presence of the corrosion inhibitor, respectively.

Using electrochemical impedance, spectra were recorded at frequency range between 30 kHz to 0.1 Hz using AC signals of amplitude 0.5 mV peak to peak. The charge

transfer resistance (R_{ct}), electrolyte resistance (R_s), and double-layer capacitance (C_{dl}) were calculated via the non-linear fitting of Nyquist plots to Randle's theoretical equivalent circuit. The inhibition efficiency was calculated from charge transfer resistance values using Eq. (2):

$$IE\% = \frac{R_{ct} - R_{ct}^{\circ}}{R_{ct}} \times 100 \quad (2)$$

where the terms R_{ct}° and R_{ct} are the charge transfer resistances in the absence and presence of inhibitor, respectively [32,33].

2.8. Statistical analysis

In comparing the corrosion inhibition efficiency of sodium alginate with that of sodium alginate grafted with polyacrylamide, paired *t*-test was carried out. Pairing of data was due to dose dependance.

2.9. Qualitative analysis of inhibition of mild steel corrosion

Changes in the surface morphology of the mild steel samples were examined using scanning electron microscope (JEOL, JSM – IT200 Series, JAPAN). Samples exposed to the corrosion acidic medium with 240 mg SAG-*g*-PAC addition for 24 h and samples without the addition of the inhibitor as control were examined to reveal presence or absence of inhibitor adsorption. Images at 1,000x magnification were photographed of control and treated samples.

3. Results and discussion

3.1. FTIR Characterization of SAG-g-PAC

The FTIR of the two spectra of acrylamide (AC) and sodium alginate (SAG) are separately shown in Fig 1. A combined sodium alginate polyacrylamide spectrum Fig. 1 emphasizes the success of sodium alginate being grafted with polyacrylamide (SAG-*g*-PAC). The shift of SAG-*g*-PAC spectrum at 3,426 cm^{-1} indicates that some interactions among the functional groups of sodium alginate and polyacrylamide have occurred. These are due to the overlapping of the OH stretching vibration peak of SAG at 3,426 cm^{-1} and the double N–H stretching vibration peak of AC at 3,356 cm^{-1}. Some additional peaks in the bio-copolymer spectrum are the peaks at 1.658 and 1.615 cm^{-1} respectively corresponding to the carbonyl amide and N–H stretching vibrations; and the peak at 1,402 cm^{-1} is due to C–N stretching vibrations. So, the presence of these additional peaks confirms the success of PAC chains being grafted onto SAG backbone [34,35].

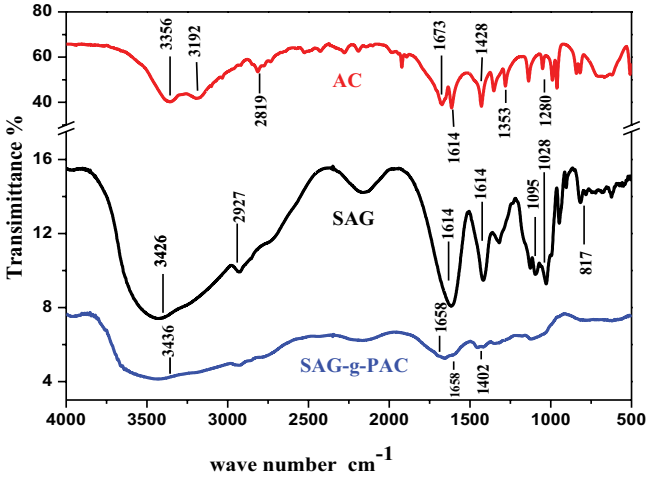

Fig. 1. FTIR spectra of acrylamide (AC), sodium alginate (SAG), and polyacrylamide grafted (SAG-*g*-PAC).

3.2. Electrochemical measurements

3.2.1. Polarization measurements

Potentiodynamic polarization curves of mild steel in 0.1 M H_2SO_4, in the presence and absence of SAG, and SAG-*g*-PAC are shown in Figs. 2 and 3. The shifting of

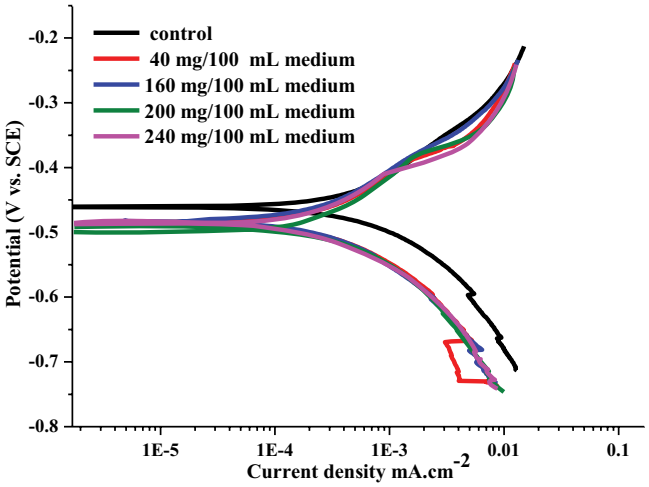

Fig. 2. Potentiodynamic polarization curves of steel in 0.1 M H_2SO_4 solution with and without addition of SAG at different concentrations (T = 298 K).

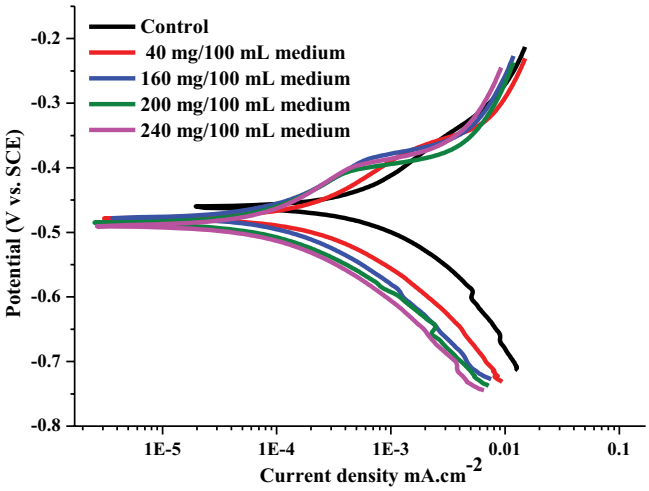

Fig. 3. Potentiodynamic polarization curves of steel in 0.1 M H_2SO_4 solution with and without addition of SAG-*g*-PAC at different concentrations (T = 298 K).

the corrosion potential (E_{corr}) to more negative values compared with control was found to be dependent on SAG, and SAG-*g*-PAC dosing. Moreover, SAG and SAG-*g*-PAC most probably act as mixed type inhibitors as E_{corr} negative shifting was less than 85 mV [36]. Dose increase caused the decrease of anodic and cathodic Tafel slopes (β_C, β_A) (Tables 1 and 2). This explained the adsorption of SAG and SAG-*g*-PAC on the metal surface which blocked the cathodic and anodic sites and retarding the cathodic hydrogen evolution reaction and reduction of the anodic dissolution of the metal [37]. Tafel parameters and the calculated inhibition efficiency (%IE) are given in Table 2. Fig. 4 shows a comparison between inhibition efficiencies of SAG and SAG-*g*-PAC. There was an increase in the corrosion inhibition efficiency with dose increase. Grafting SAG with PAC caused more than 50% increase of its inhibition efficiency (Table 2). This demonstrates the effectiveness of grafting a synthetic polymer with a natural one as to increase the number of active functional groups in the process of corrosion inhibition. Such functional groups probably caused adsorption enhancement of the inhibitor on the metal surface.

3.2.2. Electrochemical impedance spectroscopy measurements

Polarization measurements were confirmed through applying the impedance technique. Nyquist plots obtained from EIS for mild steel in 0.1 M H_2SO_4, in presence and absence of SAG, SAG-*g*-PAC inhibitors are shown in Figs. 5 and 6. The increase of inhibitors dose caused an increase in the semicircle diameter (Figs. 5 and 6). Moreover, the increase in R_{ct} values and decrease of C_{dl} values (Table 3) indicated the formation of the protective layer on the electrode/electrolyte interface and the displacing of the water molecules by SAG and SAG-*g*-PAC inhibitors [38–40]. Comparison between SAG and SAG-*g*-PAC inhibition efficiencies is illustrated in Fig. 7 and Table 3, where grafting enhanced the inhibition efficiency of SAG confirming the results of polarization technique, and the difference was statistically highly significant.

3.3. Adsorption of inhibitor on the mild steel surface

Images of the scanning electron microscopy of the mild steel surface are shown in Fig. 8A–C. Compared with blank Fig. 8A surface morphology of the mild steel immersed in 0.1 M H_2SO_4 for 24 h Fig. 8B shows severe damage, this damage was not observed in the sample immersed in acidic medium and 240 mg SAG-*g*-PAC/100 mL (Fig. 8C). This revealed adsorption of the inhibitor on the metal surface as a mechanism of protection against corrosion.

3.4. Adsorption isotherm

Surface coverage θ data obtained from the EIS of SAG and SAG-*g*-PAC were used to test the degree of fitness to different isotherm models. Fig. 9A–D give the regression and correlation results of four tested isotherm models namely Langmuir, Temkin, Flory–Huggins, and kinetic model of El-Awady isotherm. These models are expressed by the following equations [41–45]:

Table 2
Comparison of potentiodynamic polarization parameters and inhibition efficiency (IE) of mild steel in 0.1 M H_2SO_4 in the absence and presence of SAG and SAG-*g*-PAC corrosion inhibitors (T = 298 K)

Ratio mg/100 mL medium	SAG					SAG-*g*-PAC					Difference in IE (%)	Percent difference (%)
	$-E_{corr}$ (mV)	i_{corr} (μA cm^{-2})	β_A (mV dec^{-1})	β_C (mV dec^{-1})	IE[a] (%)	$-E_{corr}$ (mV)	i_{corr} (μA cm^{-2})	β_A (mV dec^{-1})	β_C (mV dec^{-1})	IE[a] (%)		
Control (0.0)	461.00	765.00	203.7	135.0	0.00	461.00	766.00	204.0	135.1	0.00	0.00	0.00
40	486.00	446.00	196.4	141.3	42	478.00	261.00	153.6	124.6	66	24	57.14
160	482.00	331.00	155.9	124.2	57	477.00	146.00	157.8	116.7	81	24	42.11
200	490.00	323.00	141.0	124.7	58	486.00	104.00	139.8	101.2	86	28	48.28
240	486.00	313.00	145.8	122.6	59	490.00	112.00	162.7	112.9	85	26	44.10

Paired student *t*-test: t_{cal} = 26.63 > t_{tab} = 4.54, p = 0.01;
[a]Values are averages of three replicas.

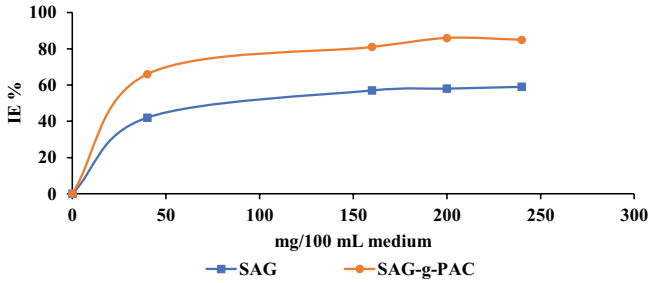

Fig. 4. Inhibition efficiency (IE) of SAG and SAG-*g*-PAC, using polarization testing technique.

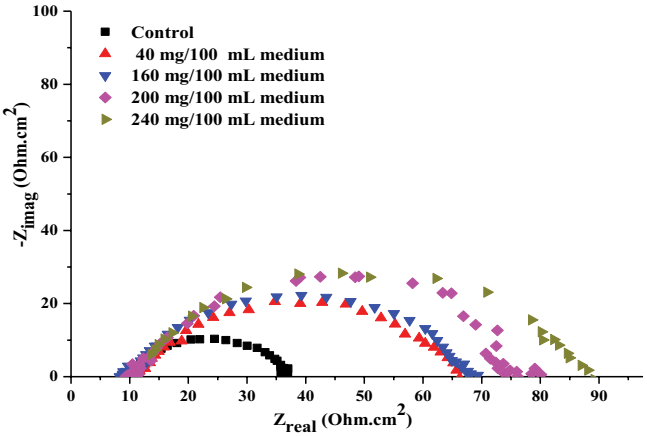

Fig. 5. Nyquist plots of steel in 0.1 M H_2SO_4 solution with and without addition of SAG at different concentrations (T = 298 K).

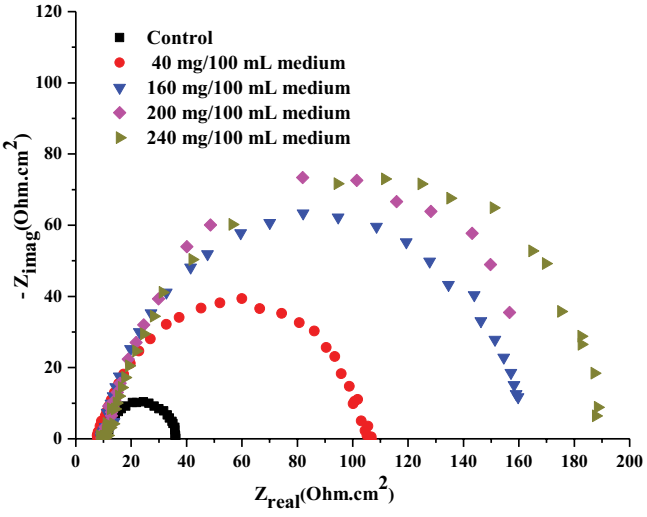

Fig. 6. Nyquist plots of steel in 0.1 M H_2SO_4 solution with and without addition of SAG-*g*-PAC at different concentrations (T = 298 K).

$$\text{Langmuir: } \frac{C}{\theta} = \frac{1}{K_{ads}} + C \quad (3)$$

$$\text{Temkin: } \theta = -\frac{1}{2a}\ln C - \frac{1}{2a}\ln K_{ads} \quad (4)$$

Table 3
Comparison of impedance parameters and inhibition efficiency (IE) of mild steel in 0.1 M H_2SO_4 in the absence and presence of SAG and SAG-*g*-PAC corrosion inhibitors (T = 298 K)

Ratio mg/100 mL medium	SAG				SAG-*g*-PAC				Difference in IE (%)	Percent difference (%)
	R_s (Ω cm^{-2})	C_{dl} (μF)	R_{ct} (Ω cm^{-2})	IE[a] (%)	R_s (Ω cm^{-2})	C_{dl} (μF)	R_{ct} (Ω cm^{-2})	IE[a] (%)		
Control (0.0)	10.70	177.30	25.40	0	10.70	177.30	25.40	0	0	0.00
40	10.73	82.93	53.00	52	8.00	65.11	93.50	73	21	40.40
160	9.50	98.52	55.00	54	10.73	50.21	149.50	83	29	53.70
200	10.50	73.68	63.00	60	10.82	56.95	170.00	85	25	41.70
240	14.00	77.15	70.00	64	10.85	51.93	163.00	86	22	34.40

Paired student *t*-test: t_{cal} = 13.49 > t_{tab} = 4.54, p = 0.01;
[a]Values are averages of three replicas.

$$\text{Florry} - \text{Huggins: } \log\frac{\theta}{C} = \log xK + x\log\left(1-\theta\right) \quad (5)$$

$$\text{Kinetic model of El-Awady isotherm: } \log\frac{\theta}{1-\theta} = y\log C + \log K,\ K_{ads} = K^{\frac{1}{y}} \quad (6)$$

where θ is the surface coverage, K_{ads} is the adsorption–desorption equilibrium constant, C is the inhibitor ratio, a is the molecular interaction parameter, x is the size parameter, which is a measure of the number of adsorbed water molecules substituted by a given inhibitor molecule, and y represents the number of inhibitor molecules occupying one active site of the metal surface. When $1/y > 1$ this means that each inhibitor molecule occupies more than one active site on the metal surface.

SAG data fitted well with Langmuir isotherm giving a good fit linear regression line with a correlation coefficient 0.9795 (Fig. 9A). This was not the case with other isotherm models. On the other hand, SAG-*g*-PAC data fitted well with the four tested models (Fig. 9A–D). Linear regression relationship and correlation coefficients higher than 0.99 were obtained. This indicated that grafting SAG with PAC polymer changed its properties as a corrosion inhibitor. This change was also manifested in the significant difference in the inhibition efficiency, as SAG-*g*-PAC gave higher inhibition efficiency than SAG. More functional groups, such as NH_2 and the oxygenated hetero atoms could be the reason for higher adsorption of the inhibitor on the metal surface. The high correlation coefficient R^2 obtained for SAG-*g*-PAC data when tested against the different isotherms mentioned above indicated a good fit of the data with such isotherm models. In such case, one can assume that grafting SAG with PAC promoted adsorption of the corrosion inhibitor on the metal surface. Values of the calculated different adsorption models' parameters are shown in Table 4. The molecular interaction parameter (a) of Temkin model was found negative which indicated that there was a repulsion between the adsorbed inhibitor molecules. While the size parameter (x) of Flory–Huggins model which is known as a substitution model was found equal to 2.20 indicating that 2.20 water molecules were substituted by one inhibitor molecule in sulfuric acid medium. This was also confirmed by the kinetic model of El-Awady isotherm as $1/y$ was found greater than one which implied that SAG-*g*-PAC molecule occupies more than one active site on the mild steel surface [44].

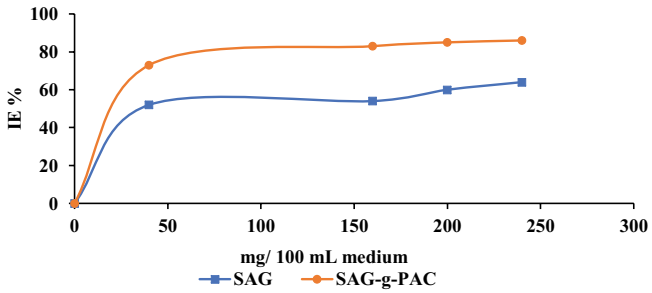

Fig. 7. Inhibition efficiency (IE) of SAG and SAG-*g*-PAC, using impedance testing technique.

3.5. Free energy of adsorption (ΔG_{ads})

The equilibrium constant of adsorption (K_{ads}) of SAG-*g*-PAC on the surface of mild steel is related to the free energy of adsorption (ΔG_{ads}) according to Eq. (7).

$$\Delta G_{ads} = -RT\ln\left(K_{ads} \times C_{solvent}\right) \quad (7)$$

where R (8.314 JK mol^{-1}) is the gas constant and T (298 K) is the absolute temperature, and $C_{solvent}$ is the concentration of solvent (water fraction is 999 g/L). Table 4 summarizes K_{ads} and ΔG_{ads} values of each isotherm model. The results showed that free energy of adsorption ΔG_{ads} was negative and less than –20 kJ mol^{-1}. This indicated that adsorption either SAG or SAG-*g*-PAC on mild steel surface is spontaneous and occurred according to the mechanism of physical adsorption [43]. This revealed that the adsorption took place by electrostatic interaction between the charged metal surface and the charged inhibitor molecules.

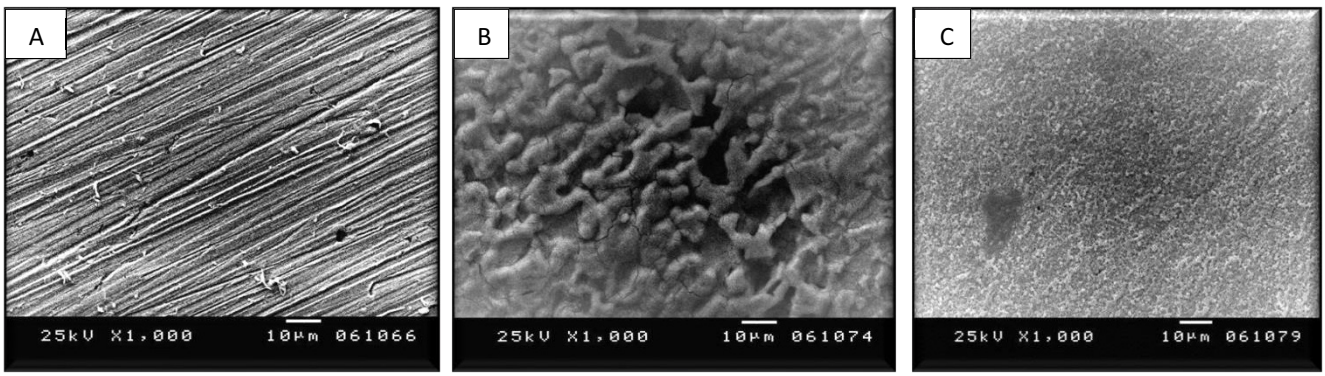

Fig. 8. Scanning electron microscopy images (A) mild steel (blank), (B) mild steel in 0.1 M H_2SO_4 (control) and (C) mild steel with 240 mg/100 mL of SAG-*g*-PAC for 24 h.

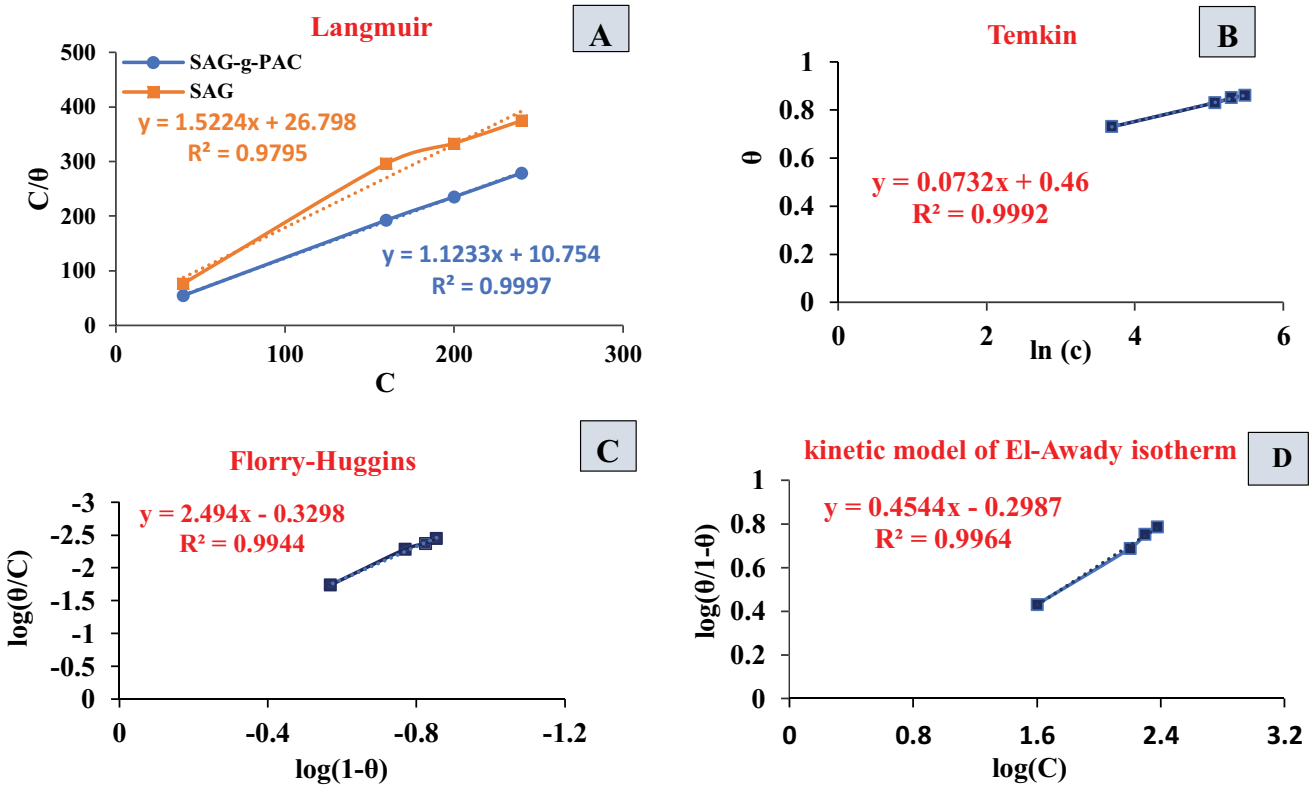

Fig. 9. Different adsorption isotherm models (A) Langmuir for SAG and SAG-*g*-PAC, (B) Temkin, (C) Flory–Huggins and (D) kinetic model of El-Awady isotherm for SAG-*g*-PAC on the surface of mild the steel in acidic medium at 298 K.

Table 4
Isotherm model parameters values

Isotherm model	Inhibitor	Model parameters values				
		K_{ads} [a]	*a*	*X*	1/*y*	ΔG_{ads} [b] (kJ/mol)
Langmuir	SAG	0.037	–	–	–	–1.78
	SAG-*g*-PAC	0.093	–	–	–	–4.07
Temkin	SAG	?	?	?	?	?
	SAG-*g*-PAC	1.17	–6.83	–	–	–10.34
Flory–Huggins	SAG	?	?	?	?	?
	SAG-*g*-PAC	0.22	–	2.49	–	
Kinetic model of El-Awady isotherm	SAG	?	?	?	?	?
	SAG-*g*-PAC	0.86	–	–	2.20	–9.57

[a]K_{ads} = Adsorption equilibrium constant;
[b]ΔG_{ads} = Free energy of adsorption kJ/mol;
? = Poor correlation, does not fit model;
– Not applicable.

3.6. Mechanism of inhibition

SAG-*g*-PAC backbone have a number of functional groups –OH, –NH_2, and oxygen hetero atoms (Fig. 10) that can interact chemically, physically or both to form a protective film insulating the metal surface from the corroding medium. Physical interaction arises from the electrostatic interaction between the metal surface and the charged inhibitor. While chemical interaction arises from the interaction between the unshared electron pairs of heteroatoms and the d-orbitals of the metal surface to form a new bond [43]. Since the data obtained from the studied adsorption models and free energy ΔG_{ads} which was found to be <–20 kJ mol^{-1} indicating that adsorption took place by a physical adsorption process. In Table 5, some data from the literature are reported. The cited papers addressed the increase of corrosion inhibition efficiency of different corrosion inhibitors due to grafting with polyacrylamide

Table 5
Comparison between enhancement of mild steel corrosion inhibition efficiency

Inhibitor	Corrosion medium	Concentration/ Ratio (mg L^{-1})	Efficiency of corrosion inhibition %		Increase %	Ref. No.
			Grafting			
			Before	After		
Pectin-grafted polyacrylamide (Pec-g-PAAm)	3.5% NaCl	800	73	85	16	27
Grafting of polyacrylamide with Okra mucilage (O-g-PAM)	0.5 M H_2SO_4	100	72	96	33	28
Xanthan gum-graft-polyacrylamide (XG-g-PAM)	15% HCl	500	90	93	3	25
Gum acacia-graft-polyacrylamide (GA-g-PAM)	15% HCl	300	84	93	10	24
Polyacrylamide grafted guar gum (GG-g-PAM)	1 M HCl	500	71	91	28	26
Sodium alginate grafted with polyacrylamide (SAG-*g*-PAC)	0.1 M H_2SO_4	2,400	64	86	34	Present work

Electrochemically measured achieved in our work and similar published works.

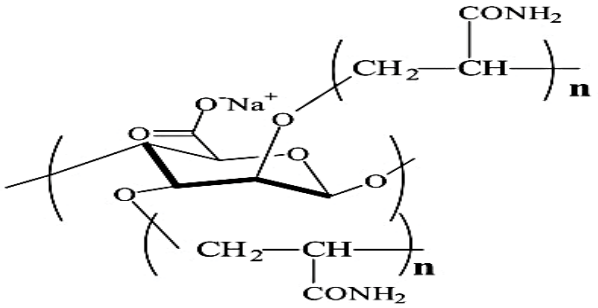

Fig. 10. Structure of sodium alginate grafted with polyacrylamide (SAG-*g*-PAC).

(PAC) [24–28]. It is noticeable that the present work achieved a 34% increase of corrosion inhibition efficiency via grafting sodium alginate with polyacrylamide which is the highest among all cited similar data.

4. Conclusion

The enhancement of corrosion inhibition efficiency of SAG after grafting with PAC was highly significant. Polarization measurements revealed that SAG-*g*-PAC biocopolymer acted as mixed type inhibitor. Inhibition efficiency values obtained from impedance are in good agreement with polarization results. The FTIR spectra of SAG-*g*-PAC showed the presence of functional groups containing heteroatoms which probably why grafting increased inhibition efficiency, particularly via adsorption. The qualitative analysis showed that the inhibitor adsorption forms a protective film on the mild steel surface. The adsorption of SAG-*g*-PAC on the mild steel in 0.1 M H_2SO_4 obeyed more than one model namely Langmuir, Temkin, Flory–Huggins, and kinetic model of El-Awady isotherm, while SAG obeyed Langmuir model only. The values of ΔG_{ads} indicated that SAG-*g*-PAC follows the physisorption adsorption mechanism.

References

[1] N. Hossain, M.A. Chowdhury, M. Kchaou, An overview of green corrosion inhibitors for sustainable and environment friendly industrial development, J. Adhes. Sci. Technol., 35 (2021) 673–690.
[2] A. Miralrio, A.E. Vázquez, Plant extracts as green corrosion inhibitors for different metal surfaces and corrosive media: a review, Processes, 8 (2020) 942, doi: 10.3390/PR8080942.
[3] F. Habashi, History of corrosion research, CIM Bull., 96 (2003) 88–94.
[4] N. Raghavendra, Latest exploration on natural corrosion inhibitors for industrial important metals in hostile fluid environments: a comprehensive overview, J. Bio- Tribo-Corrosion, 5 (2019) 1–19, doi: 10.1007/s40735-019-0240-x.
[5] F. Darriet, M. Znini, L. Majidi, A. Museli, B. Hammouti, A. Bouyanzer, J. Costa, Evaluation of *Eryngium maritimum* essential oil as environmentally friendly corrosion inhibitor for mild steel in hydrochloric acid solution, Int. J. Electrochem. Sci., 8 (2013) 4328–4345.
[6] M.N. El-Haddad, Chitosan as a green inhibitor for copper corrosion in acidic medium, Int. J. Biol. Macromol., 55 (2013) 142–149.
[7] A. Jmiai, B. El Ibrahimi, A. Tara, S. El Issami, O. Jbara, L. Bazzi, Alginate biopolymer as green corrosion inhibitor for copper in 1 M hydrochloric acid: experimental and theoretical approaches, J. Mol. Struct., 1157 (2018) 408–417.
[8] E. Khamis, E. El-Rafey, A.M. Abdel Gaber, A. Hefnawy, N.G. El-Din Shams El-Din, M.S. El-Din Esmail Ahmed, Comparative study between green and red algae in the control of corrosion and deposition of scale in water systems, Desal. Water Treat., 57 (2016) 23571–23588.
[9] H. Wei, B. Heidarshenas, L. Zhou, G. Hussain, Q. Li, K. (Ken) Ostrikov, Green inhibitors for steel corrosion in acidic environment: state of art, Mater. Today Sustainability, 10 (2020) 100044, doi: 10.1016/j.mtsust.2020.100044.
[10] C. Verma, E.E. Ebenso, I. Bahadur, M.A. Quraishi, An overview on plant extracts as environmental sustainable and green corrosion inhibitors for metals and alloys in aggressive corrosive media, J. Mol. Liq., 266 (2018) 577–590.

[11] L.T. Popoola, Organic green corrosion inhibitors (OGCIs): a critical review, Corros. Rev., 37 (2019) 71–102.
[12] S.A. Umoren, U.M. Eduok, Application of carbohydrate polymers as corrosion inhibitors for metal substrates in different media: a review, Carbohydr. Polym., 140 (2016) 314–341.
[13] A. Jmiai, B. El Ibrahimi, A. Tara, I. Bazzi, R. Oukhrib, S. El Issami, O. Jbara, L. Bazzi, M. Hilali, The effect of the two biopolymers "sodium alginate and chitosan" on the inhibition of copper corrosion in 1 M hydrochloric acid, Mater. Today:. Proc., 22 (2020) 12–15.
[14] I.B. Obot, I.B. Onyeachu, A. Madhan Kumar, Sodium alginate: a promising biopolymer for corrosion protection of API X60 high strength carbon steel in saline medium, Carbohydr. Polym., 178 (2017) 200–208.
[15] N. Dang, Y.H. Wei, L.F. Hou, Y.G. Li, C.L. Guo, Investigation of the inhibition effect of the environmentally friendly inhibitor sodium alginate on magnesium alloy in sodium chloride solution, Mater. Corros., 66 (2015) 1354–1362.
[16] S.M. Tawfik, Alginate surfactant derivatives as an ecofriendly corrosion inhibitor for carbon steel in acidic environments, RSC Adv., 5 (2015) 104535–104550.
[17] R. Hassan, I. Zaafarany, A. Gobouri, H. Takagi, A revisit to the corrosion inhibition of aluminum in aqueous alkaline solutions by water-soluble alginates and pectates as anionic polyelectrolyte inhibitors, Int. J. Corros., 2013 (2013) 508596, doi: 10.1155/2013/508596.
[18] I. Braccini, S. Pérez, Molecular basis of Ca^{2+}-induced gelation in alginates and pectins: the egg-box model revisited, Biomacromolecules, 2 (2001) 1089–1096.
[19] K.Y. Lee, D.J. Mooney, Alginate: properties and biomedical applications, Prog. Polym. Sci., 37 (2012) 106–126.
[20] E.M.S. Azzam, H.M.A. El-Salam, R.A. Mohamed, S.M. Shaban, A. Shokry, Control the corrosion of mild steel using synthesized polymers based on polyacrylamide, Egypt. J. Pet., 27 (2018) 897–910.
[21] A. Ali Fathima Sabirneeza, R. Geethanjali, S. Subhashini, Polymeric corrosion inhibitors for iron and its alloys: a review, Chem. Eng. Commun., 202 (2015) 232–244.
[22] B. Yao, G. Wang, J. Ye, X. Li, Corrosion inhibition of carbon steel by polyaniline nanofibers, Mater. Lett., 62 (2008) 1775–1778.
[23] C. Wang, C. Zou, Y. Cao, Electrochemical and isothermal adsorption studies on corrosion inhibition performance of β-cyclodextrin grafted polyacrylamide for X80 steel in oil and gas production, J. Mol. Struct., 1228 (2021) 129737, doi: 10.1016/j.molstruc.2020.129737.
[24] A. Biswas, P. Mourya, D. Mondal, S. Pal, G. Udayabhanu, Grafting effect of gum acacia on mild steel corrosion in acidic medium: gravimetric and electrochemical study, J. Mol. Liq., 251 (2018) 470–479.
[25] A. Biswas, S. Pal, G. Udayabhanu, Experimental and theoretical studies of xanthan gum and its graft co-polymer as corrosion inhibitor for mild steel in 15% HCl, Appl. Surf. Sci., 353 (2015) 173–183.
[26] P. Roy, P. Karfa, U. Adhikari, D. Sukul, Corrosion inhibition of mild steel in acidic medium by polyacrylamide grafted guar gum with various grafting percentage: effect of intramolecular synergism, Corros. Sci., 88 (2014) 246–253.
[27] R. Geethanjali, A. Ali Fathima Sabirneeza, S. Subhashini, Water-soluble and biodegradable pectin-grafted polyacrylamide and pectin-grafted polyacrylic acid: electrochemical investigation of corrosion-inhibition behaviour on mild steel in 3.5% NaCl media, Indian J. Mater. Sci., 2014 (2014) 356075, doi: 10.1155/2014/356075.
[28] S. Banerjee, V. Srivastava, M.M. Singh, Chemically modified natural polysaccharide as green corrosion inhibitor for mild steel in acidic medium, Corros. Sci., 59 (2012) 35–41.
[29] V. Srivastava, S. Banerjee, M.M. Singh, Inhibitive effect of polyacrylamide grafted with fenugreek mucilage on corrosion of mild steel in 0.5 M H_2SO_4 at 35°C, J. Appl. Polym. Sci., 116 (2010) 810–816.
[30] V. Singh, P. Kumar, R. Sanghi, Use of microwave irradiation in the grafting modification of the polysaccharides – a review, Prog. Polym. Sci., 37 (2012) 340–364.
[31] P. Rani, S. Mishra, G. Sen, Microwave based synthesis of polymethyl methacrylate grafted sodium alginate: its application as flocculant, Carbohydr. Polym., 91 (2013) 686–692.
[32] H.A. Fetouh, A. Hefnawy, A.M. Attia, E. Ali, Facile and low-cost green synthesis of eco-friendly chitosan-silver nanocomposite as novel and promising corrosion inhibitor for mild steel in chilled water circuits, J. Mol. Liq., 319 (2020) 114355, doi: 10.1016/j.molliq.2020.114355.
[33] X. Li, S. Deng, H. Fu, Inhibition of the corrosion of steel in HCl, H_2SO_4 solutions by bamboo leaf extract, Corros. Sci., 62 (2012) 163–175.
[34] J.M.C. Da Feira, J.M. Klein, M.M. De Camargo Forte, Ultrasound-assisted synthesis of polyacrylamide-grafted sodium alginate and its application in dye removal, Polimeros, 28 (2018) 139–146.
[35] G. Sen, R.P. Singh, S. Pal, Microwave-initiated synthesis of polyacrylamide grafted sodium alginate: synthesis and characterization, J. Appl. Polym. Sci., 115 (2010) 63–71.
[36] F.M. Mahgoub, A.M. Hefnawy, E.H. Abd Alrazzaq, Corrosion inhibition of mild steel in acidic solution by leaves and stem extract of acacia nilotica, Desal. Water Treat., 169 (2019) 49–58.
[37] Q.H. Zhang, B.S. Hou, Y.Y. Li, G.Y. Zhu, H.F. Liu, G.A. Zhang, Two novel chitosan derivatives as high efficient eco-friendly inhibitors for the corrosion of mild steel in acidic solution, Corros. Sci., 164 (2020) 108346, doi: 10.1016/j.corsci.2019.108346.
[38] M. Faiz, A. Zahari, K. Awang, H. Hussin, Corrosion inhibition on mild steel in 1 M HCl solution by: *Cryptocarya nigra* extracts and three of its constituents (alkaloids), RSC Adv., 10 (2020) 6547–6562.
[39] P. Kong, H. Feng, N. Chen, Y. Lu, S. Li, P. Wang, Polyaniline/chitosan as a corrosion inhibitor for mild steel in acidic medium, RSC Adv., 9 (2019) 9211–9217.
[40] C. Jeyaprabha, S. Sathiyanarayanan, G. Venkatachari, Polyaniline as corrosion inhibitor for iron in acid solutions, J. Appl. Polym. Sci., 101 (2006) 2144–2153.
[41] O.A. Akinbulumo, O.J. Odejobi, E.L. Odekanle, Thermodynamics and adsorption study of the corrosion inhibition of mild steel by *Euphorbia heterophylla* L. extract in 1.5 M HCl, Results Mater., 5 (2020) 100074, doi: 10.1016/j.rinma.2020.100074.
[42] S.A. Xavier Stango, U. Vijayalakshmi, Studies on corrosion inhibitory effect and adsorption behavior of waste materials on mild steel in acidic medium, J. Asian Ceram. Soc., 6 (2018) 20–29.
[43] E. Ituen, O. Akaranta, A. James, Evaluation of performance of corrosion inhibitors using adsorption isotherm models: an overview, Chem. Sci. Int. J., 18 (2017) 1–34.
[44] Z.V.P. Murthy, K. Vijayaragavan, Mild steel corrosion inhibition by acid extract of leaves of *Hibiscus sabdariffa* as a green corrosion inhibitor and sorption behavior, Green Chem. Lett. Rev., 7 (2014) 209–219.
[45] J.T. Nwabanne, V.N. Okafor, Adsorption and thermodynamics study of the inhibition of corrosion of mild steel in H_2SO_4 medium using *Vernonia amygdalina*, J. Miner. Mater. Charact. Eng., 11 (2012) 885–890.